THE JOURNAL OF BIOLOGICAL CHEMISTRY VOL. 285, NO. 1, pp. 576–582, January 1, 2010

CD38-mediated Ca^{2+} Signaling Contributes to Angiotensin II-induced Activation of Hepatic Stellate Cells

*ATTENUATION OF HEPATIC FIBROSIS BY CD38 ABLATION**

Received for publication, October 14, 2009 Published, JBC Papers in Press, November 12, 2009, DOI 10.1074/jbc.M109.076216

Seon-Young Kim[‡1], **Baik Hwan Cho**[§], **and Uh-Hyun Kim**[‡¶2]

From the Departments of [‡]*Biochemistry and* [§]*Surgery and the* [¶]*Institute of Cardiovascular Research, Chonbuk National University Medical School, Jeonju 561-182, Republic of Korea*

CD38 is a type II glycoprotein that is responsible for the synthesis and hydrolysis of cyclic ADP-ribose (cADPR) and nicotinic acid adenine dinucleotide phosphate (NAADP), Ca^{2+}-mobilizing second messengers. The activation of hepatic stellate cells (HSCs) is a critical event in hepatic fibrosis because these cells are the main producers of extracellular matrix proteins in the liver. Recent evidence indicates that the renin-angiotensin system plays a major role in liver fibrosis. In this study, we showed that angiotensin II (Ang II) evoked long lasting Ca^{2+} rises and induced NAADP or cADPR productions via CD38 in HSCs. Inositol 1,4,5-trisphosphate as well as NAADP-induced initial Ca^{2+} transients were prerequisite for the production of cADPR, which was responsible for later sustained Ca^{2+} rises in the Ang II-treated HSCs. Ang II-mediated inositol 1,4,5-trisphosphate- and NAADP-stimulated Ca^{2+} signals cross-talked in a dependent manner with each other. We also demonstrated that CD38 plays an important role in Ang II-induced proliferation and overproduction of extracellular matrix proteins in HSCs, which were reduced by an antagonistic cADPR analog, 8-bromo-cADPR, or in $CD38^{-/-}$ HSCs. Moreover, we presented evidence to implicate CD38 in the bile duct ligation-induced liver fibrogenesis; infiltration of inflammatory cells and expressions of α-smooth muscle actin, transforming growth factor-β1, collagen αI(1), and fibronectin were reduced in $CD38^{-/-}$ mice compared with those in $CD38^{+/+}$ mice. These results demonstrate that CD38-mediated Ca^{2+} signals contribute to liver fibrosis via HSCs activation, suggesting that intervention of CD38 activation may help prevent hepatic fibrosis.

Hepatic fibrosis represents a major medical problem worldwide with significant morbidity and mortality. Chronic stimuli like alcohol consumption, viral infection, cholestasis, or metabolic disorders result in the deposition of scar tissue and the development of cirrhosis. Hepatic stellate cells (HSCs)[3] are the major players during liver fibrogenesis (1). Upon liver injury, normally quiescent HSCs become activated, undergo profound morphological changes, and transdifferentiate into myofibroblast-like cells. This process is termed "HSC activation," in which *de novo* expression of α-smooth muscle actin (SMA), enhanced cell proliferation, and excessive production of extracellular matrix (ECM) are the most characteristic features (2). HSCs are activated by a variety of hormones or growth factors, including angiotensin II (Ang II) (3–6). There is evidence that the renin-angiotensin system components are up-regulated in HSCs isolated from human cirrhotic livers and in cultured HSCs (7). Moreover, previous studies have revealed that an activated HSC expresses Ang II type 1 receptor (7), and blockade of Ang II type 1 receptor has been shown to attenuate hepatic fibrosis in an animal model (8). Furthermore, therapeutic efficacy of an Ang II type 1 receptor blocker in a patient with nonalcoholic steatohepatitis has also been reported (9).

Cells possess multiple Ca^{2+} stores and multiple Ca^{2+}-mobilizing messenger molecules (10–13). These include inositol 1,4,5-trisphosphate (IP_3), cyclic adenosine diphosphoribose (cADPR), and nicotinic acid adenine dinucleotide phosphate (NAADP). It is generally accepted that Ca^{2+} stores for IP_3 and cADPR are located in endoplasmic reticulum (ER) in most mammalian cells, whereas Ca^{2+} stores for NAADP are localized in acidic organelles (11–13). The IP_3 receptor (IP_3R) and receptor for cADPR (ryanodine receptor) have been well characterized (13, 14); however, one isoform of two-pore channels (TPC2) has recently been proposed as a receptor for NAADP (15). Intriguingly, the receptor for NAADP has a property of desensitization with a high concentration of NAADP (16). The multifunctional ectoenzyme CD38 synthesizes cADPR and NAADP (17). Recently, CD38 was identified as a key regulator of HSC activation (18). However, the precise mechanism underlying the association between CD38 and HSC activation in liver fibrosis remains to be resolved.

In this study, we studied whether Ang II-mediated CD38 activation can induce an increase of intracellular Ca^{2+} concentration ($[Ca^{2+}]_i$) in HSCs via NAADP and/or cADPR production, ECM protein accumulation, and proliferation. We also attempted to elucidate the mechanism of CD38 involvement in Ang II-induced HSC activation and evaluated preventive potential of genetic ablation of CD38 in the development and

* This work was supported by a grant of the Korea Healthcare Technology R&D Project, Ministry for Health, Welfare & Family Affairs, Republic of Korea (A090476; to U.-H. K.).

[1] A BK21 recipient at Chonbuk National University.

[2] To whom correspondence should be addressed: Dept. of Biochemistry, Chonbuk National University, Medical School, Keum-am dong, Jeonju 561-182, Republic of Korea. Tel.: 82-63-270-3083; Fax: 82-63-274-9833; E-mail: uhkim@chonbuk.ac.kr.

[3] The abbreviations used are: HSC, hepatic stellate cell; Ang II, angiotensin II; HCS, hepatic stellate cells; cADPR, cyclic ADP-ribose; NAADP, nicotinic acid adenine dinucleotide phosphate; IP_3, inositol 1,4,5-trisphosphate; BDL, bile duct ligation; α-SMA, α-smooth muscle actin; TGF-β1, transforming growth factor β1; ECM, extracellular matrix; ER, endoplasmic reticulum; Col-I, collagen αI(1); Br, bromo.

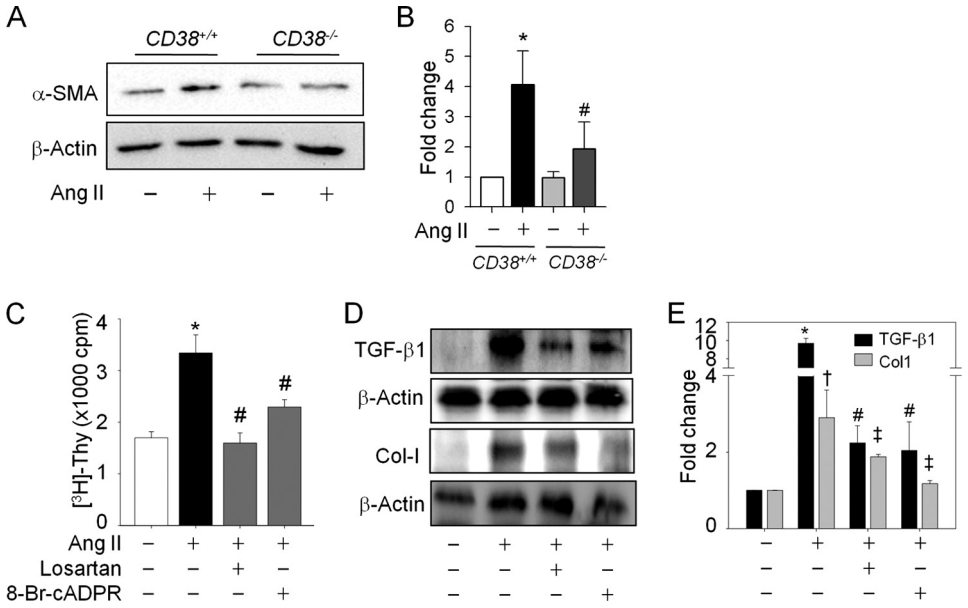

FIGURE 1. **Ang II-induced CD38 activation is the main mediator of HSC activation, proliferation, and collagen αI(1) expression.** *A*, expression of α-SMA in $CD38^{+/+}$ or $CD38^{-/-}$ HSCs after Ang II (100 nM) treatment for 48 h. β-Actin was used to evaluate equal protein loading. *B*, relative expression of α-SMA expression is arbitrarily presented. *, $p < 0.001$ *versus* control in $CD38^{+/+}$ HSCs; #, $p < 0.01$ *versus* Ang II in $CD38^{+/+}$ HSCs. *C*, Ang II-induced DNA synthesis was blocked by losartan (10 μM) and 8-Br-cADPR (100 μM) pretreatment. HSCs were treated with Ang II (100 nM) for 48 h after pretreatment of each inhibitor. *, $p < 0.001$ *versus* control; #, $p < 0.01$ *versus* Ang II. *D* and *E*, TGF-β1 and Col-I expression were changed in response to Ang II in the presence of losartan and 8-Br-cADPR. *, $p < 0.001$ *versus* control; #, $p < 0.05$ *versus* Ang II. Values are means ± S.E. of three independent experiments. *Thy*, thymidine; *cpm*, counts per minutes.

progression of liver fibrosis in a mouse model induced by bile duct ligation (BDL).

EXPERIMENTAL PROCEDURES

Animals and Materials—All animal experiments and materials were described. C57BL/6J and $CD38^{-/-}$ male mice were purchased from The Jackson Laboratory (Bar Harbor, ME). All animals received humane care in compliance with the guidelines from the Animal Care and Use Committee of Chonbuk National University. Ang II, 8-Br-cADPR, bafilomycin A1, nicotinamide guanine dinucleotide (NGD^+), and other chemicals were purchased from Sigma-Aldrich. Xestosphonsin C (XeC) was purchased from Calbiochem, and losartan was purchased from Merck.

Animal Treatments—Liver fibrosis was induced in two-month-old $CD38^{-/-}$ or $CD38^{+/+}$ male mice by BDL, as described previously (9). Briefly, after a midline laparotomy, the common bile duct was doubly ligated by 4-0 silk and transected between the two ligations. The sham operation was similarly performed except the bile duct was not ligated and transected. Mice were randomized to undergo a BDL or sham operation. Six mice were used in each group. All animals were sacrificed 4 weeks after surgery, and blood and liver samples were obtained.

Serum Biochemical Measurements—Serum alanine aminotransferase, aspartate aminotransferase, and alkaline phosphatase activities were measured using the diagnostic kit (Sigma) following manufacturer's instructions. Their activity was detected on an ultraviolet/visible scanning spectrophotometer (Beckman DU-640, Beckman Instrument, Inc., Fullerton, CA).

Isolation of Mouse Stellate Cells—Mouse hepatic stellate cells were isolated as described previously (8). In brief, livers of 6- to 8-week-old male mice (20–25 g body mass) were perfused first with a Ca^{2+}/Mg^{2+}-free solution (137 mM NaCl, 5.4 mM KCl, 0.6 mM $NaH_2PO_4 \cdot 2H_2O$, 0.8 mM $Na_2HPO_4 \cdot 12H_2O$, 10 mM Hepes, 0.5 mM EGTA, 4.2 mM $NaHCO_3$, and 5 mM glucose, pH 7.4) at 37 °C and next with 0.015% collagenase A (Roche Applied Science) and 0.1% Pronase E (Roche Applied Science) solution (137 mM NaC1, 5.4 mM KC1, 0.6 mM $NaH_2PO_4 \cdot 2H_2O$, 0.8 mM $Na_2HPO_4 \cdot 12H_2O$, 3.8 mM $CaCl_2$, 10 mM Hepes, 4.2 mM $NaHCO_3$, pH 7.4) at 37 °C. The digested liver was excised, dispersed in Ca^{2+}/Mg^{2+}-free solution, and filtered through gauzes. Residual hepatocytes were removed twice by a low speed centrifugation (50 × *g*, 4 °C, 2 min). The nonparenchymal cells were pelleted by centrifugation (450 × *g*, 4 °C, 10 min). A stellate cell-enriched fraction was obtained by the use of centrifugation with a triple-layered (9, 11, and 17%) Nycodenz cushion (Sigma-Aldrich, 1,400 × *g*, 4 °C, 20 min). The cells in the upper layer were washed by centrifugation (450 × *g*, 4 °C, 10 min) and suspended in Dulbecco's modified Eagle's medium (Invitrogen) supplemented with 10% fetal calf serum (Invitrogen) and antibiotics. After plating, the culture medium was changed every other day.

[^{3}H]Thymidine Incorporation Assay—DNA synthesis was measured by the incorporation of methyl-[^{3}H]thymidine (Amersham Biosciences) as described previously (19). Before measuring the incorporation, HSCs were pretreated with 8-Br-cADPR or losartan for 30 min and then incubated with Ang II for 24 h. HSCs were then incubated in the same medium with 1.0 μCi/ml [^{3}H]thymidine for 6 h at 37 °C. The cells were then washed once with phosphate-buffered saline treated with ice-cold 5% trichloroacetic acid at 4 °C for 15 min, and then washed twice in 5% trichloroacetic acid. The acid-insoluble material was dissolved in 2 N NaOH at room temperature and counted for radioactivity by liquid scintillation counting. All experiments were performed in triplicate.

Immunoblotting—Whole-cell extracts and liver extracts were prepared as described previously (19). Proteins (20 μg/lane) were resolved on 8 or 12% SDS-PAGE gel and transferred to polyvinylidine difluoride membranes (GE Healthcare). Antibodies against α-SMA (DakoCytomation, Carpentaria, CA), TGF-β1, collagen αI(1) (Col-I), and fibronectin (Santa Cruz Biotechnology, Santa Cruz, CA) were used. Horseradish peroxide-conjugated secondary antibodies (Santa Cruz Biotechnology) were used and visualized using enhanced

chemiluminescence. All immunoreactive signals were analyzed by densitometric scanning (Fuji Photo Film Co., Tokyo, Japan).

Measurement of $[Ca^{2+}]_i$—The measurement method is described. Changes of $[Ca^{2+}]_i$ in HSCs were determined as described previously (20). HSCs grown to near confluence were made quiescent by serum deprivation overnight at 37 °C. Serum-starved cells were incubated with 5 μM Fluo-3 AM (Molecular Probes) in Hank's balanced salt solution (2 mM $CaCl_2$, 145 mM NaCl, 5 mM KCl, 1 mM $MgCl_2$, 5 mM D-glucose, and 20 mM HEPES, pH 7.3) at 37 °C for 40 min. The cells were washed three times with Hank's balanced salt solution. Changes of $[Ca^{2+}]_i$ were determined at 488 nm excitation/530 nm emission by air-cooled argon laser system. The emitted fluorescence at 530 nm was collected using a photomultiplier. The image was scanned using a confocal microscope (Nikon). For the calculation of $[Ca^{2+}]_i$, the method of Tsien *et al.* (21) was used with the following equation: $[Ca^{2+}]_i = K_d(F - F_{min})/(F_{max} - F)$, where K_d is 450 nM for fluo-3, and F is the observed fluorescence level. Each tracing was calibrated for the maximal intensity (F_{max}) by addition of ionomycin (8 μM) and for the minimal intensity (F_{min}) by addition of EGTA 50 mM at the end of each measurement.

Measurement of Intracellular cADPR Concentration—The sample extraction was performed as described previously (20, 21). cADPR was measured by some modification of the cycling method described previously (20). Briefly, cells were treated with 0.3 ml of 0.6 M-perchloric acid under sonication. Precipitates were removed by centrifugation at 20,000 × *g* for 10 min. Perchloric acid was removed by mixing the aqueous sample with a solution containing 3 volumes of 1,1,2-trichlorotrifluoroethane to 1 volume of tri-*n*-octylamine. After centrifugation for 10 min at 1,500 × *g*, the aqueous layer was collected and neutralized with 20 mM sodium phosphate pH 8.0. To remove all contaminating nucleotides, the samples were incubated with the following hydrolytic enzymes overnight at 37 °C: 0.44 unit/ml nucleotide pyrophosphatase, 12.5 units/ml alkaline phosphatase, 0.0625 units/ml NAD glycohydrolase, and 2.5 mM $MgCl_2$ in 20 mM sodium phosphate buffer, pH 8.0. Enzymes were removed by filtration using a Centricon-3 filter (Amicon). To convert cADPR to β-NAD^+, the samples (0.1 ml/tube) were incubated with 50 μl of cycling reagent containing 0.3 μg/ml Aplysia ADP-ribosyl cyclase, 30 mM nicotinamide, and 100 mM sodium phosphate, pH 8.0, at room temperature for 30 min. The samples were further incubated with the cycling reagent (0.1 ml) containing 2% ethanol, 100 μg/ml alcohol dehydrogenase, 20 μM resazurin, 10 μg/ml diaphorase, 10 μM riboflavin 5′-phosphate, 10 mM nicotinamide, 0.1 mg/ml BSA, and 100 mM sodium phosphate, pH 8.0, at room temperature for 2 h. An increase in the resorufin fluorescence was measured at an excitation of 544 nm and an emission of 590 nm using a SpectraMax gemini fluorescence plate reader (Molecular Devices Corp.). Various known concentrations of cADPR were also included in the cycling reaction to generate a standard curve.

Measurement of Intracellular NAADP Concentration—The level of NAADP was measured using a cyclic enzymatic assay as described previously (21).

Measurement of IP_3—Intracellular IP_3 was measured as described previously (22). Briefly, HSCs were incubated with

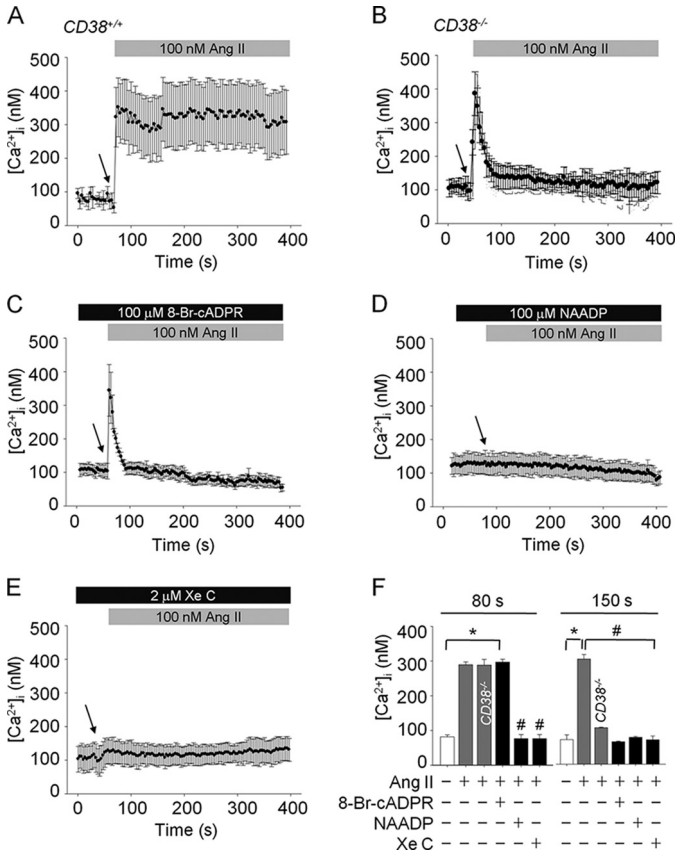

FIGURE 2. **Ang II-evoked $[Ca^{2+}]_i$ rise is mediated by IP_3/NAADP/cADPR.** *A*, increases of $[Ca^{2+}]_i$ by Ang II in $CD38^{+/+}$ HSCs. *B*, the later phase of $[Ca^{2+}]_i$ was abolished in $CD38^{-/-}$ HSCs by Ang II. *C*, Ang II-mediated sustained $[Ca^{2+}]_i$ increases were inhibited by pretreatment with 8-Br-cADPR (100 μM). *D* and *E*, pretreatment of HSCs with NAADP (100 μM) and XeC (2 μM) completely blocked Ang II-induced $[Ca^{2+}]_i$. *F*, changes in $[Ca^{2+}]_i$ at 80 and 150 s. *, $p < 0.001$ *versus* basal $[Ca^{2+}]_i$; #, $p < 0.05$ *versus* Ang II. Values are means ± S.E. of three independent experiments. The *arrow* indicates the time of Ang II addition.

[^{3}H]inositol (PerkinElmer Life Sciences, 0.4 μCi/ml) in inositol-free Dulbecco's modified Eagle's medium for 40–48 h. Prior to assay, the medium was removed and the cells were incubated in phosphate-buffered saline containing 10 mM lithium for 10 min. The assay was initiated by the addition of test compounds and terminated after incubation at 37 °C for 20 min by the addition of 1 ml of ch1oroform:methanol:HCl (100:200:2). To separate the phases, 0.3 ml each of chloroform and 0.1 N HCl were added. The aqueous phase was subjected to chromatography on Dowex AG 1-X8 (formate form). Total inositol phosphates (sum of inositol monophosphate, inositol bisphosphate, and inositol trisphosphate) were eluted.

Histological Analysis—Formalin-fixed liver tissues were decalcified in EDTA for 5–7 days, dehydrated, and embedded in paraffin. Serial sections (4 μm) were stained with hematoxylin-eosin. The extent of inflammation was evaluated on blinded slides by digital images using a computer-assisted color image analyzer (LUZEX F, Nikon, Tokyo, Japan).

Immunohistochemistry—Tissue sections were cut and placed on glass slides, deparaffinized with xylene, and rehydrated with graded ethanol. Endogenous peroxidase was blocked with 3% hydrogen peroxide for 20 min, and slides were rinsed with phosphate-buffered saline. After protein blocking, slides were incubated overnight at 4 °C with a primary antibody for α-SMA

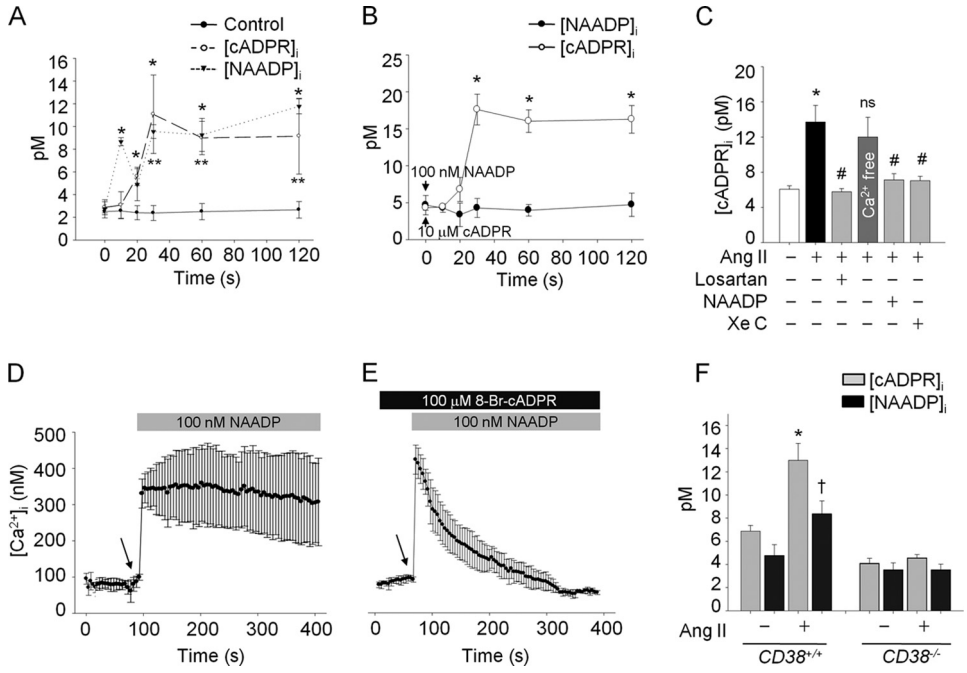

FIGURE 3. **NAADP-induced [Ca^{2+}]$_i$ stimulates cADPR production by Ang II in HSCs.** *A*, kinetics of cADPR and NAADP production by Ang II in CD38$^{+/+}$ HSCs. *, $p < 0.05$ *versus* basal intracellular cADPR concentration ([cADPR]$_i$); **, $p < 0.05$ *versus* basal intracellular NAADP concentration ([NAADP]$_i$). *B*, exogenous cADPR0-mediated (10 μM) or NAADP-mediated (100 nM) [NAADP]$_i$ or [cADPR]$_i$ increase in CD38$^{+/+}$ HSCs is presented in a time course. *, $p < 0.01$ *versus* basal [cADPR]$_i$. *C*, Ang II-mediated cADPR production was inhibited by losartan, XeC, and a high concentration of NAADP, but not in the absence of extracelluar Ca^{2+}. *D*, NAADP-induced (100 nM) increase of [Ca^{2+}]$_i$ in HSCs. *E*, NAADP-evoked sustained Ca^{2+} increase was abolished in the presence of 8-Br-cADPR. *F*, Ang II-stimulated cADPR or NAADP production was measured in CD38$^{-/-}$ HSCs. *, $p < 0.001$ *versus* basal [cADPR]$_i$; †, $p < 0.05$ *versus* basal [NAADP]$_i$. Values are means ± S.E. of three independent experiments.

(1:100; DakoCytomation). The stained sections were then incubated with biotinylated secondary antibody (DakoCytomation), and the immune complexes were detected using an ABC kit according to manufacturer's instructions. The sections were finally counterstained with hematoxylin before mounting. The area of positive staining was determined by computerized image analysis (LUZEX F, Nikon).

Statistical Analysis—Data represent means ± S.E. of at least three separate experiments. Statistical comparisons were performed using one-way analysis of variance followed by Scheffe's test. Statistical significance of difference between groups was determined using Student's *t* test. Differences were considered significant if the *p* value was <0.05.

RESULTS

Ang II-mediated cADPR Production by CD38 Is Essential in HSC Activation, Proliferation, and ECM Protein Accumulation—Because α-SMA is a sensitive marker of activated HSCs *in situ*, it has increasingly been used as an early indicator of fibrogenetic activity in human liver disease, even before ECM accumulates (23). To elucidate a possibility of an association between CD38 and HSC activation in liver fibrosis, we compared the α-SMA expression in HSCs isolated from CD38$^{+/+}$ and CD38$^{-/-}$ mice after 48 h of treatment with Ang II. As seen in Fig. 1, *A* and *B*, the increase of α-SMA protein in CD38$^{-/-}$ HSCs in response to Ang II was consistently lower than in CD38$^{+/+}$ HSCs. Treatment of HSCs with Ang II stimulated proliferative responses as demonstrated by an increase in [^{3}H]thymidine uptake (Fig. 1*C*). Pretreatment of HSCs for 30 min with 8-Br-cADPR, an antagonistic analog of cADPR, significantly inhibited Ang II-induced DNA synthesis. We also confirmed the inhibitory effect of losartan, an Ang II type 1 receptor blocker, on HSCs proliferation. Ang II treatment up-regulated TGF-β1 and Col-I levels and that these up-regulations were abrogated by pretreatment of HSCs with 8-BrcADPR or losartan (Fig. 1, *D* and *E*).

CD38 Ablation Attenuates Ang II-induced Sustained Intracellular Ca^{2+} Increases in HSCs—To explore the role of CD38 in Ang II-mediated Ca^{2+} signaling in HSCs, we compared Ca^{2+} signaling in HSCs from CD38$^{+/+}$ and CD38$^{-/-}$ mice. Ang II evoked sustained intracellular Ca^{2+} increase in CD38$^{+/+}$ HSCs; however, the later phase of sustained Ca^{2+} signal was not detected in the Ang II-treated HSCs from CD38$^{-/-}$ mice (Fig. 2, *A* and *B*). Pretreatment of HSCs with 8-Br-cADPR blocked the sustained Ca^{2+} increase, similar to that shown in CD38$^{-/-}$ HSCs (Fig. 2*C*), suggesting that Ang II-mediated long lasting Ca^{2+} signaling in HSCs is due to the action of cADPR. Pretreatment of HSCs with high concentration of NAADP or XeC, an IP_3R blocker, led to a complete blockade of the Ang II-induced intracellular Ca^{2+} response, including initial Ca^{2+} transient in HSCs (Fig. 2, *D* and *E*). Thus, the Ang II-mediated Ca^{2+} signal in HSCs consists of two phases of Ca^{2+} signals; initial Ca^{2+} transient is dependent on both IP_3 and NAADP, whereas later sustained Ca^{2+} signal on cADPR (Fig. 2*F*).

Ang II Stimulates cADPR Production following NAADP Production in HSCs—To elucidate whether cADPR and NAADP are produced in Ang II-treated HSCs, we measured intracellular cADPR or NAADP concentrations before and after treatment of HSCs with Ang II. As shown in Fig. 3*A*, NAADP was produced ~10 s earlier than cADPR with its initial peak at 10 s following Ang II treatment, and the levels of NAADP and cADPR were sustained with similar patterns until 120 s. Moreover, exogenous NAADP evoked cADPR production directly in HSCs, whereas exogenous cADPR did not induce NAADP production (Fig. 3*B*), indicating that NAADP-mediated initial Ca^{2+} increase is required for cADPR production. Ang II-mediated cADPR production was blocked by pretreatment of the cells with high concentrations of NAADP, XeC, and losartan, but not by the Ca^{2+}-free condition (Fig. 3*C*). Therefore, it is highly likely that exogenous NAADP could induce a Ca^{2+} signal similar to that of Ang II-mediated Ca^{2+} increase in HSCs. Indeed, NAADP was found to elicit a Ca^{2+} increase similar to

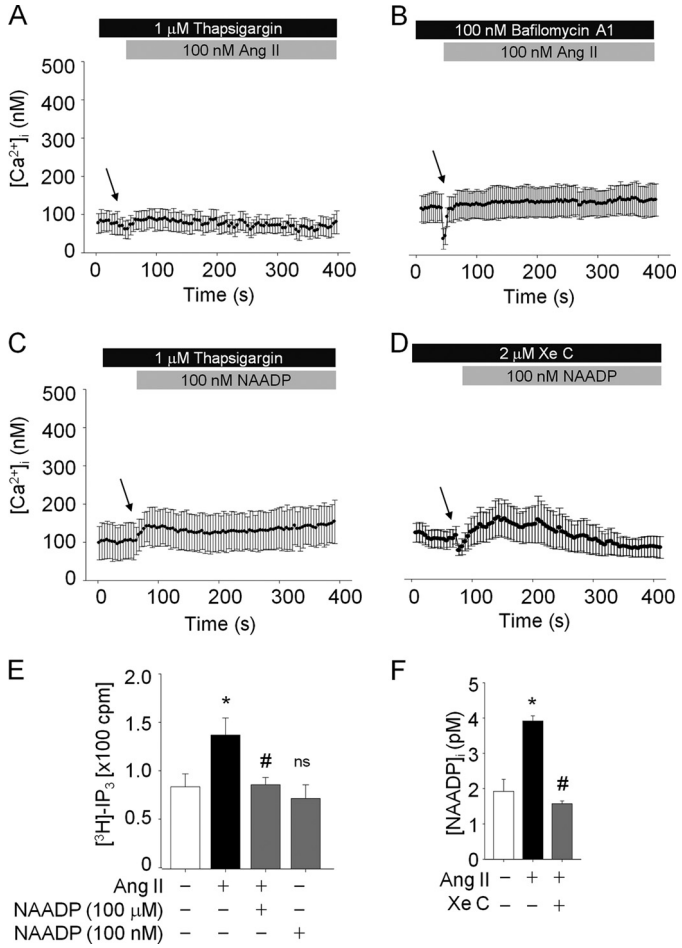

FIGURE 4. **NAADP- or IP_3-induced Ca^{2+} signals closely interact in Ang II-mediated mechanism.** *A* and *B*, thapsigargin and bafilomycin A1 abolished Ang II-evoked Ca^{2+} increase. *C* and *D*, NAADP failed to increase $[Ca^{2+}]_i$ in the presence of thapsigargin and XeC. *E*, Ang II-stimulated IP_3 synthesis was blocked in the presence of a high concentration of NAADP (100 μM). Exogenous NAADP (100 nM) did not affect IP_3 production. High concentration of NAADP (100 μM) was preincubated prior to Ang II treatment. Ang II (100 nM) or NAADP (100 nM) was treated for 15 s. *, $p < 0.01$ *versus* basal [^{3}H]-IP_3; #, $p < 0.05$ *versus* Ang II. *F*, Ang II-induced NAADP production was inhibited by XeC pretreatment. *, $p < 0.01$ *versus* basal $[NAADP]_i$; #, $p < 0.01$ *versus* Ang II; ns, non-significant. Values are means ± S.E. of three independent experiments.

that of Ang II-treated HSCs (Fig. 3*D*). Pretreatment of HSCs with 8-Br-cADPR blocked the NAADP-induced late phase of long-lasting Ca^{2+} increase, but not initial Ca^{2+} signal (Fig. 3*E*). Next, we examined whether Ang II-induced cADPR or NAADP production in HSCs is due to CD38, and therefore, we compared cADPR and NAADP production in HSCs from $CD38^{+/+}$ and $CD38^{-/-}$ mice before and after treatment with Ang II. HSCs from $CD38^{-/-}$ mice did not produce cADPR as well as NAADP in response to Ang II (Fig. 3*F*), indicating that CD38 is responsible for the production of cADPR and NAADP HSCs in response to Ang II.

Characterization of the Ang II-induced Initial Phase of Ca^{2+} Signals in HSCs—Figs. 2 and 3 show that NAADP and IP_3 contributed to initial phase of Ca^{2+} increase and cADPR formation in the Ang II-treated HSCs. When the Ca^{2+} pool in the ER was emptied by inhibiting the sarcoplasmic/endoplasmic reticulum Ca^{2+} ATPase pumps with thapsigargin, the Ang II-induced Ca^{2+} increase was not detected (Fig. 4*A*). In addition, bafilomycin A1, which is known to block the vacuolar H^+ ATPase (24), also completely prevented Ang II-mediated Ca^{2+} increases (Fig. 4*B*). Fig. 4, *C* and *D* show that the NAADP-evoked Ca^{2+} response was blocked by pretreatment of the cells with thapsigargin as well as XeC. These findings suggest that the NAADP-mediated Ca^{2+} signal requires IP_3-induced Ca^{2+} release from ER, and the IP_3-mediated Ca^{2+} signal requires NAADP-induced Ca^{2+} release from the acidic store. Therefore, we tested the effect of a high concentration of NAADP on Ang II-mediated intracellular IP_3 production and the effect of IP_3R blocker on NAADP formation induced by Ang II. After pretreatment with a high concentration of NAADP for 30 min, Ang II was unable to induce intracellular IP_3 increase (Fig. 4*E*). Furthermore, in the presence of IP_3R blocker, Ang II did not induce NAADP production in HSCs (Fig. 4*F*). These data indicate that Ang II-mediated IP_3 production can be affected by NAADP-induced Ca^{2+} increase and that Ang II-mediated NAADP production depends also on IP_3-mediated Ca^{2+} release in HSCs. Taken together, these results suggest that NAADP and IP_3-elicited Ca^{2+} releases from the acidic organelles and ER Ca^{2+} stores, respectively, have a cross-talk in the Ang II-mediated Ca^{2+} signals in HSCs.

TABLE 1
Comparison of liver enzymes in bile duct-ligated $CD38^{+/+}$ and $CD38^{-/-}$ mice

	Sham		BDL	
	$CD38^{+/+}$	$CD38^{-/-}$	$CD38^{+/+}$	$CD38^{-/-}$
ALT (U/L)[a]	30.56 ± 6.43	30.64 ± 3.33	347.98 ± 66.94[b]	290.20 ± 34.11
AST (U/L)	72.81 ± 10.56	76.96 ± 6.74	282.07 ± 58.20[b]	180.10 ± 43.68[c]
ALP (U/L)	50.00 ± 3.96	48.92 ± 5.94	141.64 ± 13.68[b]	110.07 ± 7.90[c]

[a] ALT, alanine aminotransferase; AST, aspartate aminotransferase; ALP, alkaline phosphatase; U/L, units per liter.
[b] $p < 0.01$ compared with the sham-operated $CD38^{+/+}$ mice group.
[c] $p < 0.05$ compared with the bile duct-ligated $CD38^{+/+}$ mice group. Values are means ± S.E.

Liver Fibrosis Is Markedly Attenuated in $CD38^{-/-}$ Mice after BDL—Because blockade of the Ang II receptor has been previously reported to attenuate BDL-induced hepatic fibrosis and our present findings showed that Ang II receptor signaling in HSCs was mediated by CD38, we examined the role of CD38 played in liver fibrosis, by applying the BDL-induced fibrosis model in $CD38^{+/+}$ and $CD38^{-/-}$ mice. Following BDL for 4 weeks, the degree of liver injury was attenuated in $CD38^{-/-}$ mice, as demonstrated by lower serum liver enzymes levels (Table 1) and lower hepatocytes necrosis and inflammatory cell infiltration than those in $CD38^{+/+}$ mice (Fig. 5*A*). Because α-SMA is primarily responsible for the overproduction of ECM at pathogenic conditions and also indicates HSC activation, we investigated the activation of HSCs by assessing the expression after BDL. Fig. 5*B* illustrates the expression of hepatic α-SMA protein in sham and BDL livers of $CD38^{+/+}$ and $CD38^{-/-}$ mice. Compared with sham controls, α-SMA expression in the BDL-$CD38^{+/+}$ mice liver was markedly increased, suggesting the activation of hepatic myofibroblasts following BDL-induced injury. However, the induction of α-SMA in the ligated $CD38^{-/-}$ mice liver was largely blocked (Fig. 5*B*). This was validated by Western blot analysis of α-SMA protein (Fig. 5, *C* and *D*). Hepatic expression of TGFβ-1, Col-I, and fibronectin in BDL-$CD38^{-/-}$ mice was significantly attenuated compared

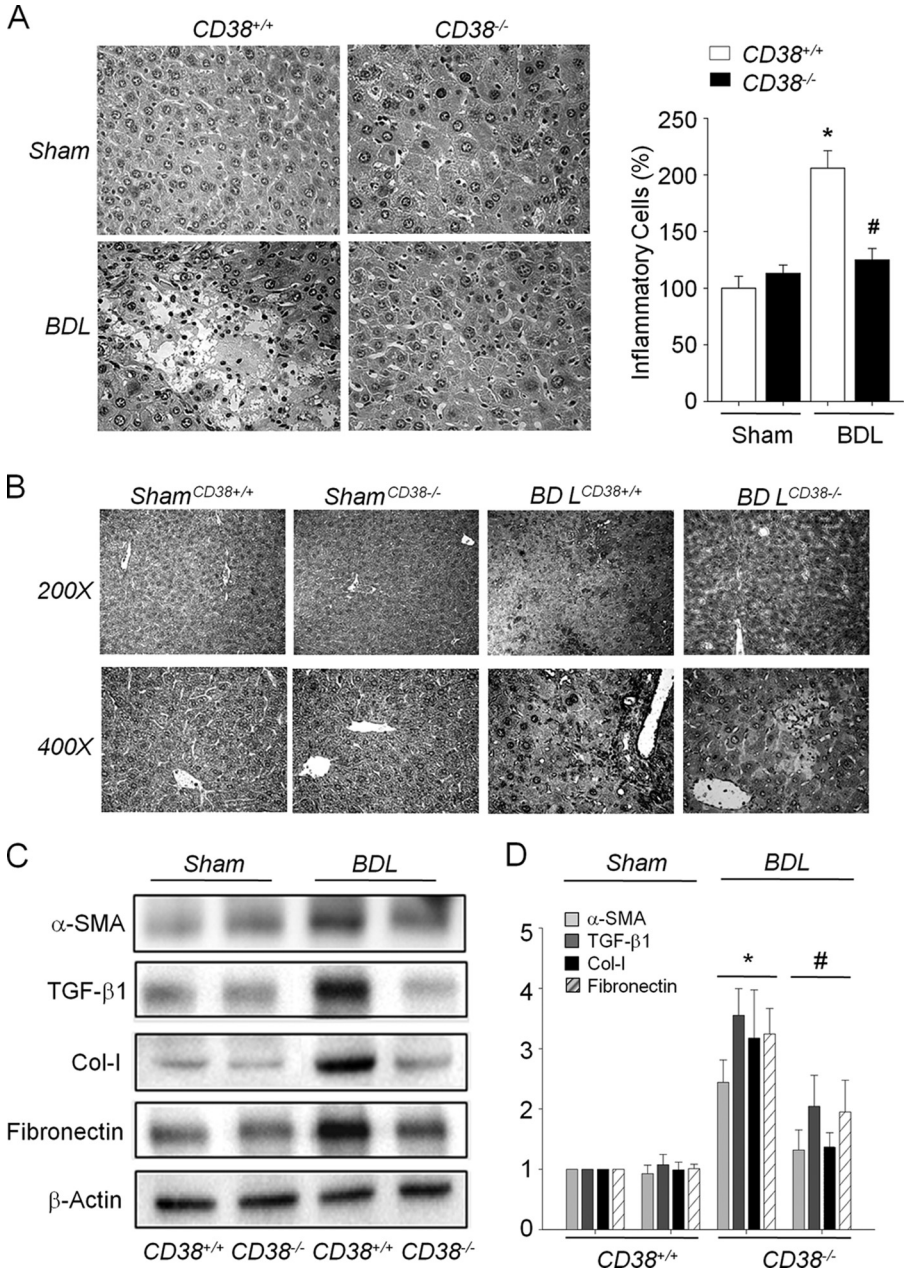

FIGURE 5. **Genetic ablation of CD38 attenuates BDL-induced liver fibrosis.** *A*, hematoxylin and eosin staining of liver specimens. BDL-induced necrosis and inflammatory cell infiltration in the liver of $CD38^{+/+}$ and $CD38^{-/-}$ mice (original magnification ×400). Quantification of inflammatory cells in liver specimens. 25 fields (×400) were studied in each liver sample. *, $p < 0.01$ *versus* in sham-operated $CD38^{+/+}$ mice liver. #, $p < 0.05$ *versus* bile duct-ligated $CD38^{+/+}$ mice liver. *B*, immunohistochemical examination of α-SMA expression in livers of $CD38^{+/+}$ and $CD38^{-/-}$ mice (original magnification ×200 on *upper panel* and ×400 on *lower panel*). *C*, comparison of expression of α-SMA, TGF-β1, Col-I, and fibronectin in the livers from $CD38^{+/+}$ and $CD38^{-/-}$ mice following BDL. *D*, relative expression of each protein compared with β-actin. *, $p < 0.01$ *versus* in sham-operated $CD38^{+/+}$ mice. #, $p < 0.05$ *versus* bile duct-ligated $CD38^{+/+}$ mice. Values are means ± S.E. of three independent experiments.

with that in $CD38^{+/+}$ mice (Fig. 5, *C* and *D*). These results indicate that CD38 is an important mediator in liver fibrosis.

DISCUSSION

A recent study documented CD38 as a regulator of activation and effector functions of HSCs (18). CD38-immunopositive HSCs were found to increase following the progression of hepatic fibrosis, which was shown in liver biopsies from patients with chronic liver disease (25). CD38 is one of the ADP-ribosyl cyclases, a family of multifunctional enzymes that are seemingly ubiquitous in eukaryotic cells, and ADP-ribosyl cyclases play a key role in several physiological processes, including cell proliferation, muscle contraction, stem cell regeneration, and hormone secretion (17). We previously reported activation mechanisms of Ang II-mediated ADP-ribosyl cyclase in mouse mesangial cells or adult rat cardiomyocytes (19, 26) and also showed that ADP-ribosyl cyclase inhibitions could provide a protective effect on chronic renal and cardiac failure (27, 28). In the present study, we proposed a link between Ang II and CD38 activation during liver fibrosis and presented evidence that Ang II induces fibrogenic actions through CD38 activation in activated HSCs. Our present results showed that the profibrogenic effect of Ang II is associated with an increased concentration of TGF-β1. Previous studies have demonstrated that Ang II induces the expression of TGF-β1 (29, 30) and that TGF-β1 has powerful fibrogenic action. By using cADPR antagonistic analogs, several laboratories have shown that cADPR regulates numerous Ca^{2+} signaling pathways in plants, invertebrates, and vertebrates (13, 31). Our present data revealed that treatment of HSCs with 8-Br-cADPR inhibited Ang II-mediated expression of TGF-β1, Col-I deposition, and cell proliferation. Furthermore, Ang II-mediated sustained Ca^{2+} increase was not observed in $CD38^{-/-}$ HSCs as well as in HSCs pretreated with 8-Br-cADPR, indicating that CD38-mediated Ca^{2+} signals regulate HSC activation, proliferation, and ECM accumulation. The present study identified an Ang II-evoked Ca^{2+} signaling in HSCs with a complex pattern of Ca^{2+} spiking induced by NAADP and IP_3. The Ang II-mediated initial phase of Ca^{2+} increase was abolished completely by either a high concentration of NAADP (100 μM), which is used to desensitize NAADP receptors (32) or by XeC, an IP_3R blocker. Furthermore, NAADP (100 nM)-induced Ca^{2+} signals as well as Ang II-induced NAADP production were blocked by XeC pretreatment. These data together with the

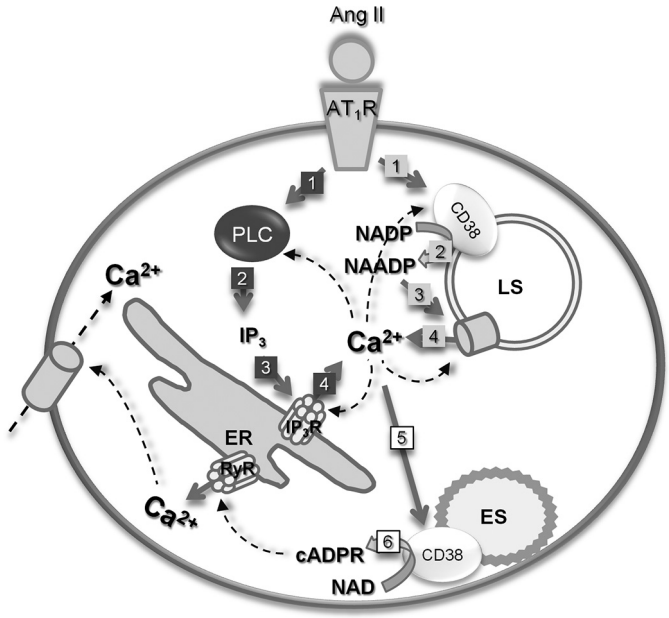

FIGURE 6. **Proposed schematic model of CD38 activation mechanism in HSCs; in HSCs, Ang II binds to the Ang II type 1 receptor and signals to activate CD38 and PLC.** Activated CD38 produces NAADP, which, in turn, stimulates Ca^{2+} release from acidic organelles. IP_3, a product of PLC, also evokes Ca^{2+} release from ER. Activations of CD38 and PLC are most likely interdependent on each Ca^{2+} signals, which, in turn, stimulate cADPR production. The *numbers* denote sequence of events. *ES*, endosome; *LS*, lysosome; *IP_3R*, IP_3 receptor; *PLC*, phospholipase C; *RyR*, ryanodine receptor.

result that NAADP-induced Ca^{2+} increase was abolished by pretreatment with thapsigargin indicate that NAADP-induced Ca^{2+} signals require ER Ca^{2+} stores and IP_3 production. Interestingly, pretreatment with bafilomycin A1 also completely blocked Ang II-mediated Ca^{2+} signals in HSCs, and Ang II in the presence of a high NAADP concentration failed to evoke IP_3 production, suggesting that IP_3R-mediated Ca^{2+} release is also dependent on NAADP-sensitive store and NAADP production. Taken together, we hypothesize that the Ang II-mediated initial phase of Ca^{2+} signals may arise through a combination of cross-talk between Ca^{2+} release from ER or acidic organelles, like Ca^{2+}-induced Ca^{2+} release and a close network between CD38 and PLC activation for the production of NAADP or IP_3 (Fig. 6). In the Ang II-treated HSCs, as we have demonstrated in other cells, cADPR was responsible for the later sustained Ca^{2+} rises. Moreover, IP_3- as well as NAADP-induced initial Ca^{2+} transients were prerequisite for the production of cADPR because cADPR production was dependent on NAADP- as well as IP_3-induced Ca^{2+} increase. In summary, the current study explored the CD38 activation mechanisms by Ang II, which exerts fibrogenic effects in HSCs. We have demonstrated that activated CD38 modulates cell activation, proliferation, TGF-β1 expression, and collagen synthesis. Furthermore, we assessed the role of CD38 in liver fibrogenesis by applying BDL to $CD38^{-/-}$ mice because Ang II is secreted by activated HSCs, and the renin-angiotensin system is overexpressed in bile duct-ligated livers (33). Our data showed a remarkable preservation of the hepatic architecture and less fibrosis and reduced expression of α-SMA, TGF-β1, Col-I, and fibronectin following BDL in $CD38^{-/-}$ mice, compared with $CD38^{+/+}$. These *in vivo* results indicate that CD38 plays a crucial role in liver fibrosis.

REFERENCES

1. Bataller, R., and Brenner, D. A. (2001) *Semin. Liver Dis.* **21,** 437–451
2. Bataller, R., and Brenner, D. A. (2005) *J. Clin. Invest.* **115,** 209–218
3. Mao, T. K., Kimura, Y., Kenny, T. P., Branchi, A., Gishi, R. G., Van de Water, J., Kung, H. J., Friedman, S. L., and Gershwin, M. E., (2002) *Autoimmunity* **35,** 521–529
4. Breitkopf, K., Roeyen, C., Sawitza, I., Wickert, L., Floege, J., and Gressner, A. M. (2005) *Cytokine* **31,** 349–357
5. Marra, F., DeFranco, R., Grappone, C., Milani, S., Pinzani, M., Pellegrini, G., Laffi, G., and Gentilini, P. (1998) *Hepatology* **27,** 462–471
6. Bataller, R., Sancho-Bru, P., Ginès, P., Lora, J. M., Al-Garawi, A., Solé, M., Colmenero, J., Nicolás, J. M., Jiménez, W., Weich, N., Gutiérrez-Ramos, J. C., Arroyo, V., and Rodés, J. (2003) *Gastroenterology* **125,** 117–125
7. Yokohama, S., Yoneda, M., Haneda, M., Okamoto, S., Okada, M., Aso, K., Hasegawa, T., Tokusashi, Y., Miyokawa, N., and Nakamura, K. (2004) *Hepatology* **40,** 1222–1225
8. Yoshiji, H., Kuriyama, S., Yoshii, J., Ikenaka, Y., Noguchi, R., Nakatani, T., Tsujinoue, H., and Fukui, H. (2001) *Hepatology* **34,** 745–750
9. Kurikawa, N., Suga, M., Kuroda, S., Yamada, K., and Ishikawa, H. (2003) *Br. J. Pharmacol.* **139,** 1085–1094
10. Pozzan, T., Rizzuto, R., Volpe, P., and Meldolesi, J. (1994) *Physiol. Rev.* **74,** 595–636
11. da Silva, C. P., and Guse, A. H. (2000) *Biochim. Biophys. Acta* **1498,** 122–133
12. Churchill, G. C., Okada, Y., Thomas, J. M., Genazzani, A. A., Patel, S., and Galione, A. (2002) *Cell* **111,** 703–708
13. Lee, H. C. (1997) *Physiol. Rev.* **77,** 1133–1164
14. Foskett, J. K., White, C., Cheung, K. H., and Mak, D. O. (2007) *Physiol. Rev.* **87,** 593–658
15. Calcraft, P. J., Ruas, M., Pan, Z., Cheng, X., Arredouani, A., Hao, X., Tang, J., Rietdorf, K., Teboul, L., Chuang, K. T., Lin, P., Xiao, R., Wang, C., Zhu, Y., Lin, Y., Wyatt, C. N., Parrington, J., Ma, J., Evans, A. M., Galione, A., and Zhu, M. X. (2009) *Nature* **459,** 596–600
16. Guse, A. H., and Lee, H. C. (2008) *Sci. Signal* **1,** re10
17. Malavasi, F., Deaglio, S., Funaro, A., Ferrero, E., Horenstein, A. L., Ortolan, E., Vaisitti, T., and Aydin, S. (2008) *Physiol. Rev.* **88,** 841–886
18. March, S., Graupera, M., Sarrias, M. R., Lozano, F., Pizcueta, P., Bosch, J., and Engel, P. (2007) *Am. J. Pathol.* **170,** 176–187
19. Kim, S. Y., Gul, R., Rah, S. Y., Kim, S. H., Park, S. K., Im, M. J., Kwon, H. J., and Kim, U. H. (2008) *Am. J. Physiol. Renal. Physiol.* **294,** F982–F989
20. Graeff, R., and Lee, H. C. (2002) *Biochem. J.* **361,** 379–384
21. Gasser, A., Bruhn, S., and Guse, A. H. (2006) *J. Biol. Chem.* **281,** 16906–16913
22. Kim, U. H., Fink, D., Jr., Kim, H. S., Park, D. J., Contreras, M. L., Guroff, G., and Rhee, S. G. (1991) *J. Biol. Chem.* **266,** 1359–1362
23. Russo, M. W., Firpi, R. J., Nelson, D. R., Schoonhoven, R., Shrestha, R., and Fried, M. W. (2005) *Liver Transplant.* **11,** 1235–1241
24. Bowman, E. J., Siebers, A., and Altendorf, K. (1988) *Proc. Natl. Acad. Sci. U.S.A.* **85,** 7972–7976
25. Abdeen, S. M., Olusi, S. O., Askar, H. A., Thalib, L., Al-Azemi, A., and George, S. (2009) *Acta Histochem.* **111,** 520–530
26. Gul, R., Kim, S. Y., Park, K. H., Kim, B. J., Kim, S. J., Im, M. J., and Kim, U. H. (2008) *Am. J. Physiol. Heart Circ. Physiol.* **295,** H77–H88
27. Kim, S. Y., Park, K. H., Gul, R., Jang, K. Y., and Kim, U. H. (2009) *Am. J. Physiol. Renal Physiol.* **296,** F291–F297
28. Gul, R., Park, J. H., Kim, S. Y., Jang, K. Y., Chae, J. K., Ko, J. K., and Kim, U. H. (2009) *Cardiovasc. Res.* **81,** 582–591
29. Castilla, A., Prieto, J., and Fausto, N. (1991) *N. Eng. J. Med.* **324,** 933–940
30. Gressner, A. M., Weiskirchen, R., Breitkopf, K., and Dooley, S. (2002) *Front. Biosci.* **7,** d793–807
31. Potter, B. V., and Walseth, T. F. (2004) *Curr. Mol. Med.* **4,** 303–311
32. Aarhus, R., Dickey, D. M., Graeff, R. M., Gee, K. R., Walseth, T. F., and Lee, H. C. (1996) *J. Biol. Chem.* **271,** 8513–8516
33. Paizis, G., Cooper, M. E., Schembri, J. M., Tikellis, C., Burrell, L. M., and Angus, P. W. (2002) *Gastroenterology* **123,** 1667–1676